TÜBİTAK

Turkish Journal of Chemistry

http://journals.tubitak.gov.tr/chem/

Research Article

Turk J Chem
(2019) 43: 651 – 662
© TÜBİTAK
doi:10.3906/kim-1806-41

# Intermolecular complexes of halocyclopropenone derivatives with the hypohalous acids HOF, HOCl, HOBr, and HOI

**Dariush MIRZAEI, Abedien ZABARDASTI*, Yaghoub MANSOURPANAH**
Department of Chemistry, Lorestan University, Khorramabad, Iran

**Received:** 14.06.2018 • **Accepted/Published Online:** 11.01.2019 • **Final Version:** 03.04.2019

**Abstract:** The intermolecular interactions between halocyclopropenone derivatives ($HC_3OX$; X = I, Br, Cl, and F) and hypohalous acids (HOY; Y = I, Br, Cl, and F) were studied via the MP2 method utilizing the aug-cc-pVTZ and aug-cc-pVTZ(-PP) basis sets. The three types of complexes were hydrogen bonds, halogen bonds, and complexes containing both hydrogen and halogen bonds. The results obtained indicated that interactions in the Type 1 complexes were stronger than those in Types 2 and 3. The H–O bonds revealed red shifts with complex formation in Types 1 and 2. The O–Y bonds displayed red shifts in the Type 3 and blue shifts in the Type 2 structures. Molecular electrostatic potential, quantum theory of atoms in molecules, and natural bond orbital methodologies were used to analyze these interactions.

**Key words:** Hydrogen bond, halogen bond, cyclopropenones, hypohalous acids

## 1. Introduction

Cyclopropenones ($C_3H_2O$) are very interesting molecules in biology and medicine as antibiotic penitricin as well as cyclopropenone-based protease inhibitors.[1,2] Cyclopropenone was first synthesized in 1967[3] and characterized by Breslow et al.[4] Cyclopropenone as the simplest aromatic molecule is a three-membered ring with $sp^2$ hybridized carbon atoms that are surprisingly stable despite its ring strain. This is probably due to the relative importance of resonance structures.[5] A number of ab initio studies have been reported for substituted cyclopropenone, $X_2C_3O$, where X = $CH_3$, F, Cl. Ab initio research on substituted $X_2C_3O$ with fluorine (X = F) indicated considerable changes in the structure, relative energies, and kinetic stability of molecules. Although the decomposition mechanism of cyclopropenones and their photochemical and thermal reactions have attracted a great deal of attention, the intermolecular interaction of cyclopropenone derivatives has not been extensively studied so far.[6–12] Noncovalent interactions are critical factors for controlling the structural and energetic aspects of molecular systems.[13–17] The hydrogen bond and halogen bond interactions as weakly noncovalent interactions with significant strength and directionality have been studied experimentally via Fourier transform microwave spectroscopy and IR detection and theoretically by ab initio and DFT calculations.[18–25] A halogen bond (XB) is an attraction between halogen atoms as electrophilic species with the nucleophilic region of an atom or molecule.[26] However, the formation of halogen bonds rarely occurs with fluoride. In response to a combination of limited polarizability and extreme electronegativity, the fluorine atom is frequently estimated not to participate in halogen bonding.[27,28] Moreover, a hydrogen bond occurs when a hydrogen atom

*Correspondence: zebardasti@yahoo.com



This work is licensed under a Creative Commons Attribution 4.0 International License.

bonds to a more electronegative atom such as F, O, and N, and another adjacent atom bearing a lone pair of electrons.[29] The hypohalous acids (HOY with Y = halogen), formed in reactions between the halogen and OH radicals in the atmosphere, have attracted particular interest due to their ability as a model for participation in a variety of intermolecular hydrogen bonds and halogen bond interactions.[30–32] This ability is related to the simultaneous presence of both the halogen donor and the proton donor in hypohalous acid. These compounds are often used as strong oxidizing agents and participate in depletion of the ozone layer, stratospheric reactions, hydroxylation, and fluorination.[33] In recent years, theoretical investigations have been reported on molecular interactions between hypohalous acids with themselves, phosphine, sulfur, formyl halides, and carbon monoxide.[34–37] These studies are useful to show the role of HOY (Y = halogen) in biological compounds and atmospheric chemistry.[38,39] The main objective of the present study was to investigate the key structure for the interactions of substituted cyclopropenones (X = halogen) with HOY molecules (Y = halogen) by the interplay between the hydrogen bond and the halogen bond. This work shows the effects of substitution of halogens on the cyclopropenone ring, its intermolecular interactions, stability of its complexes, and its structural properties. In order to investigate the nature of the interactions, quantum theory of atoms in molecules (QTAIM),[40] molecular electrostatic potential (MEP),[41] and natural bond orbital (NBO)[42] analyses were performed.

## 2. Results and discussion

### 2.1. Geometrics

Three configurations were obtained for the interaction of $HC_3OX$ with HOY molecules. Figure 1 presents a graphical illustration of the representative configurations under consideration. Possible interactions considered for HOY molecules with $HC_3OX$ include hydrogen bonding (O$\cdots$H) and halogen bonding (X$\cdots$Y, O$\cdots$X), which are denoted as XYz. X represents the cyclopropenone ($HC_3OI$, $HC_3OBr$, $HC_3OCl$, and $HC_3OF$ were specified as I, Br, Cl, and F, respectively), Y shows the HOY molecules (HOI, HOBr, HOCl, and HOF were defined as I, Br, Cl, and F, respectively), and z denotes the type of complex formed between them. For example, FI1 shows a Type 1 complex of $HC_3OF$ with HOI, while BrBr2 illustrates a Type 2 complex of $HC_3OBr$ with HOBr. The XY1 Type shows O$\cdots$H interactions, with HOY acting as a hydrogen bond donor (HBD). In the XY2 Type, the O$\cdots$H and X$\cdots$Y interactions were assigned to be between HOY and $HC_3OX$ molecules. In the H$\cdots$O interaction HOY acts as a HBD, while in the X$\cdots$Y it might act as an electron acceptor or electron donor according to the nature of X and Y atoms. For the XY3 model a halogen bond (XB) interaction was found between $HC_3OX$ and HOY in which the Y atom of HOY as an electron acceptor interacts with the O atom of $HC_3OX$ as an electron donor. It should be noted that no halogen bond was observed between $HC_3OX$ and HOF (FF3, ClF3, BrF3, and IF3). Table 1 provides the intermolecular distances for complexes and the difference in bond lengths between the complexes and the isolated monomers. The O$\cdots$H (Types 1 and 2), X$\cdots$Y, and O$\cdots$Y distances lie within the ranges of 1.762 to 1.809 Å, 1.746 to 1.823 Å, 3.064 to 4.182 Å, and 2.610 to 2.697 Å, respectively. The intermolecular distances calculated for O$\cdots$H (Types 1 and 2) and O$\cdots$Y are less than the sum of the van der Waals (vdW) radii of the corresponding atoms (vdW radii for H, O, F, Cl, Br, and I are 1.20, 1.52, 1.47, 1.75, 1.85, and 1.98 Å, respectively),[43] suggesting that an attractive force exists between the two monomers. The only exception is X$\cdots$Y, in which the distances are somewhat longer than the sum of vdW radii of the corresponding atoms, which suggests a relatively weak interaction.

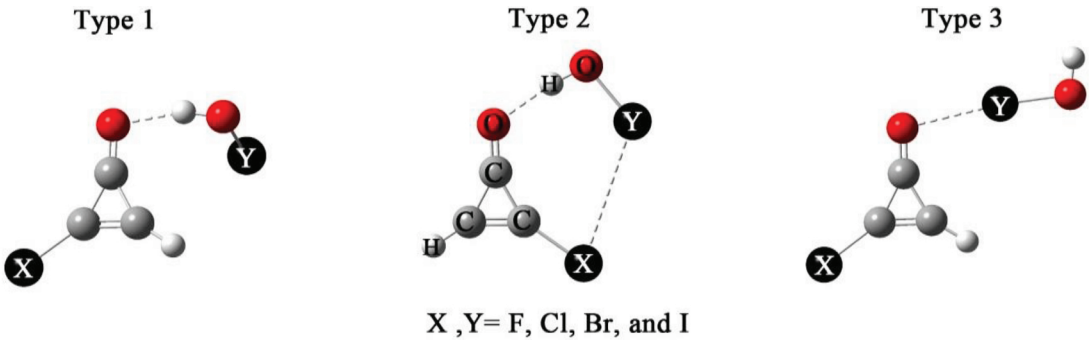


**Figure 1**. Structures of $HC_3OX\cdots HOY$ complexes.

**Table 1**. Selected geometrical parameters calculated at the MP2/aug-cc-pVTZ and MP2/aug-cc-pVTZ(-PP) levels.

| | Type 1 | | | Type 2 | | | Type 3 | | |
|---|---|---|---|---|---|---|---|---|---|
| | O···H | $\Delta r_{O-H}$ | O···H | X···Y | $\Delta r_{O-H}$ | $\Delta r_{O-Y}$ | $\Delta r_{C-X}$ | O···Y | $\Delta r_{O-Y}$ |
| FF | 1.770 | 0.017 | 1.774 | 3.064 | 0.015 | 0.005 | 0.169 | – | – |
| FCl | 1.768 | 0.018 | 1.774 | 3.474 | 0.015 | –0.004 | 0.171 | 2.697 | 0.013 |
| FBr | 1.782 | 0.017 | 1.785 | 3.542 | 0.014 | –0.009 | 0.171 | 2.633 | 0.016 |
| FI | 1.809 | 0.015 | 1.823 | 3.632 | 0.014 | 0.013 | 0.172 | 2.641 | 0.022 |
| ClF | 1.765 | 0.018 | 1.764 | 3.236 | 0.016 | 0.005 | –0.013 | – | – |
| ClCl | 1.763 | 0.019 | 1.761 | 3.653 | 0.015 | –0.004 | –0.011 | 2.687 | 0.013 |
| ClBr | 1.775 | 0.018 | 1.772 | 3.754 | 0.015 | –0.009 | –0.100 | 2.622 | 0.017 |
| ClI | 1.806 | 0.017 | 1.818 | 3.881 | 0.015 | 0.013 | –0.013 | 2.631 | 0.023 |
| BrF | 1.765 | 0.018 | 1.764 | 3.297 | 0.005 | –0.005 | –0.024 | – | – |
| BrCl | 1.762 | 0.021 | 1.761 | 3.711 | 0.009 | –0.009 | –0.021 | 2.686 | 0.013 |
| BrBr | 1.776 | 0.018 | 1.772 | 3.818 | 0.010 | –0.010 | 0.020 | 2.621 | 0.017 |
| BrI | 1.806 | 0.016 | 1.820 | 3.971 | 0.013 | 0.013 | –0.024 | 2.631 | 0.010 |
| IF | 1.755 | 0.018 | 1.749 | 3.410 | 0.018 | 0.005 | –0.008 | – | – |
| ICl | 1.751 | 0.019 | 1.746 | 3.805 | 0.021 | –0.005 | –0.005 | 2.677 | 0.014 |
| IBr | 1.764 | 0.019 | 1.761 | 3.926 | 0.018 | –0.010 | –0.005 | 2.610 | 0.018 |
| II | 1.792 | 0.017 | 1.805 | 4.182 | 0.016 | –0.013 | –0.004 | 2.625 | 0.016 |

### 2.2. MEP analysis

MEP is a well-known tool for elucidating the molecular reactive properties and the nature of intermolecular interactions. The positive regions of the MEP are associated with nucleophilic positions, while negative MEPs are indicative of electrophilic positions.[44] The three-dimensional MEP maps on the 0.001 electron/Bohr3 electron density isosurfaces of HOY (Y = halogen) and $HC_3OX$ (X = halogen) molecules are illustrated in Figure 2. As shown in this figure, for HOY, there is a positive region of MEP outside the Y atom, corresponding to the $\sigma$-hole. The most positive electrostatic potential values of the $\sigma$-hole increase in the order HOF < HOCl < HOBr. Moreover, for systems containing iodine, there is a positive region of MEP outside the Y atom. Therefore, HOY can form a halogen bond with another molecule. There is another positive region of MEP outside the hydrogen atom, which becomes more positive in the order HOBr < HOCl < HOF. This positive

region also exists in iodine-containing compounds. For $HC_3OX$, the negative region of MEP exists outside the O atom along the extension of the C=O bond. These negative regions can interact with any positive site of HOY (hydrogen and Y atoms). In addition, there are two positive regions of MEP associated with the hydrogen and X atoms.

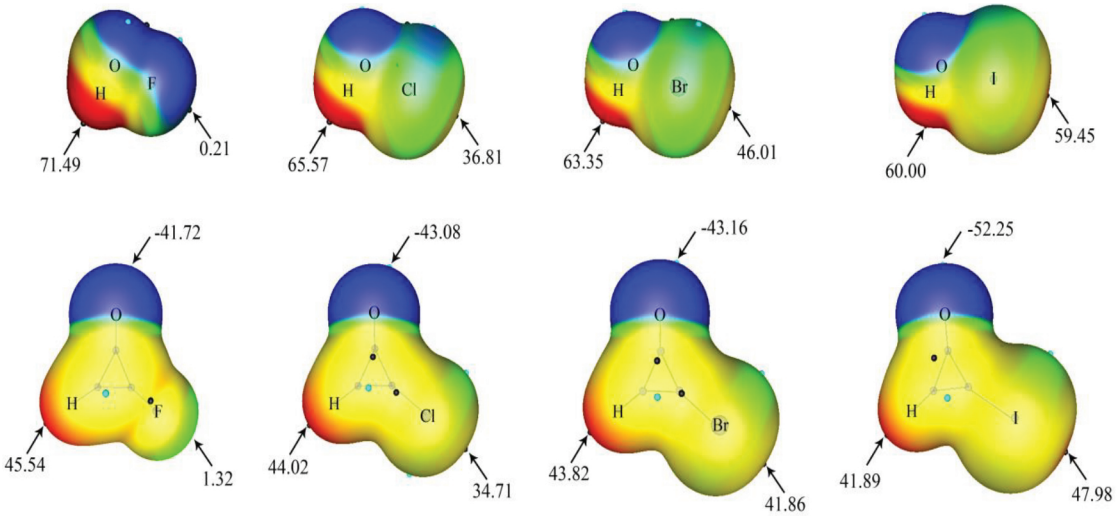


**Figure 2**. Electrostatic potential maps on the 0.001 (electron/Bohr$^3$) electron density isosurfaces of HOY (Y = F, Cl, Br, and I) and $HC_3OX$ (X = F, Cl, Br, and I) molecules. Color ranges, in kcal/mol: red > 30 > yellow > 0 > green> –10 > blue.

### 2.3. Stabilization energy

Stabilization energy (SE) is one of the most important quantities to evaluate the strength of an intermolecular interaction. Table 2 presents the SEs for the complexes of HOY (Y = halogen) and $HC_3OX$ (X = F, Cl, Br, and I) molecules. These values are corrected for zero-point energy (ZPE) and basis set superposition error (BSSE). As evident, the obtained BSSE values are about 12%–47% of the total uncorrected interaction energies. Our results show the contribution of BSSE becomes larger as the size of the Y atom increases. The $SE^{cp}$ (stabilization energy involved with corrections for both ZPE and BSSE) for Type 1, Type 2, and Type 3 complexes containing fluorine, chlorine, and bromine span a range from –6.80 to –8.20 kcal/mol, from –6.74 to –7.76 kcal/mol, and from –3.36 to –5.49 kcal/mol, respectively. Furthermore, these values for Type 1, Type 2, and Type 3 complexes containing iodine lie within the ranges of –6.13 to –7.8, –5.61 to –7.64, and –3.41 to –6.85, respectively. Therefore, for all complexes the interactions in Type 1 complexes are stronger than those in Type 2 and 3 complexes. The stabilization energies are also computed at the CCSD/aug-cc-pVTZ and CCSD/aug-cc-pVTZ(-PP) levels (see Table 2). As seen, the obtained results at the CCSD/aug-cc-pVTZ level (CCSD/aug-cc-pVTZ(-PP) level for I) are consistent with those obtained at the MP2/aug-cc-pVTZ level. This suggests that the MP2 method can be regarded as reliable to evaluate the strength and stability of halogen-bonded and hydrogen bonds systems.

### 2.4. Vibrational analysis

The changes in vibrational stretching frequencies ($cm^{-1}$) related to the HOY and $HC_3OX$ free molecules at the MP2/aug-cc-pVTZ level are shown in Tables 3 and 4. (The changes in selected vibrational stretching frequencies

**Table 2**. Uncorrected stabilization energy $SE^{uncor}$, BSSE, and $SE^{cp}$ (SE corrected with $\Delta$ZPE and BSSE) in kcal $mol^{-1}$ at the MP2/aug-cc-pVTZ and MP2/aug-cc-pVTZ(-PP) levels (values in parentheses are for CCSD/aug-cc-pVTZ and CCSD/aug-cc-pVTZ(-PP) levels).

| | Type 1 | | | | Type 2 | | | | Type 3 | | | |
|---|---|---|---|---|---|---|---|---|---|---|---|---|
| | $SE_{uncorr}$ | ΔZPE | BSSE | $SE_{cp}$ | $SE_{uncorr}$ | ΔZPE | BSSE | $SE_{cp}$ | $SE_{uncorr}$ | ΔZPE | BSSE | $SE_{cp}$ |
| FF | −9.85(−9.87) | 1.69 | 0.96 | −7.20 | −9.32 (−9.39) | 1.66 | 0.92 | −6.74 | – | – | – | – |
| FCl | −10.19(−9.33) | 1.67 | 1.11 | −7.40 | −9.84(−8.89) | 1.57 | 0.98 | −7.29 | −4.65(−3.50) | 0.71 | 0.58 | −3.36 |
| FBr | −10.58(−9.47) | 1.66 | 1.73 | −7.20 | −9.72(−8.92) | 1.52 | 1.46 | −6.74 | −7.18(−5.60) | 0.82 | 1.56 | −4.8 |
| FI | −12.39(−11.39) | 1.75 | 4.51 | −6.13 | −11.51(−8.30) | 1.67 | 4.23 | −5.61 | −11.63(−8.16) | 0.77 | 4.51 | −6.35 |
| ClF | −9.99(−10.00) | 1.66 | 0.97 | −7.36 | −9.73(−9.66) | 1.04 | 0.93 | −7.76 | – | | – | – |
| ClCl | −10.38(−9.49) | 1.05 | 1.13 | −8.20 | −9.95(−9.10) | 0.95 | 1.2 | −7.8 | −4.16(−3.54) | 0.11 | 0.59 | −3.46 |
| ClBr | −10.81(−9.64) | 1.04 | 1.76 | −8.01 | −10.14(−9.09) | 0.90 | 1.48 | −7.76 | −6.79(−5.72) | 0.21 | 1.11 | −5.47 |
| ClI | −12.79(−9.19) | 1.14 | 4.78 | −6.87 | −12.55(−8.65) | 1.09 | 4.78 | −6.59 | −11.49(−8.36) | 0.27 | 4.67 | −6.85 |
| BrF | −10.11(−10.13) | 1.67 | 1.11 | −7.33 | −9.91(−9.83) | 1.63 | 0.98 | −7.3 | – | – | – | – |
| BrCl | −10.55(−9.64) | 1.66 | 1.29 | −7.60 | −10.19(−9.27) | 1.54 | 1.20 | −7.45 | −4.86(−3.63) | 0.71 | 0.68 | −3.47 |
| BrBr | −10.99(−9.80) | 1.64 | 1.94 | −7.41 | −10.39(−9.25) | 1.49 | 1.69 | −7.21 | −7.51(−5.83) | 0.82 | 1.71 | −4.98 |
| BrI | −12.92(−9.36) | 1.72 | 4.91 | −6.29 | −12.78(−8.97) | 1.67 | 4.91 | −6.19 | −12.13(−8.50) | 0.85 | 5.69 | −5.59 |
| IF | −10.79(−10.53) | 1.64 | 1.66 | −7.49 | −10.65(−10.43) | 1.62 | 1.50 | −6.94 | – | – | – | – |
| ICl | −11.32(−10.06) | 1.60 | 1.92 | −7.8 | −10.93(−9.84) | 1.48 | 1.81 | −7.64 | −5.28(−3.98) | 0.78 | 1.06 | −3.41 |
| IBr | −11.75(−10.22) | 1.62 | 2.57 | −7.56 | −11.05(−9.83) | 1.53 | 2.25 | −7.27 | −8.00(−6.20) | 0.70 | 2.12 | −5.18 |
| II | −12.78(−11.75) | 1.67 | 4.31 | −6.80 | −12.99(−10.74) | 1.62 | 4.81 | −6.56 | −12.33(−8.15) | 0.80 | 5.70 | −5.83 |

$SE^{cp} = SE^{uncorr} + \Delta ZPE + BSSE$

($cm^{-1}$) related to the complexes obtained at the MP2/aug-cc-pVTZ level are given in Table S1, supplementary information). The C=O and H–O bonds show red shifts with complex formation for the XY1 model compared to the original bonds. In Type 1 complexes, the greatest red shift ($cm^{-1}$) is attributed to the O–H bonds of the HOY (Y = F, Cl, Br, and I) molecule and these shifts are in agreement with the order found for stabilities of complexes. In XY2 Type (X, Y = F, Cl, Br), there are red shifts related to the O–H (–275 to –326) and C=O (–8 to –22) bands. Moreover, in these complexes for systems containing iodine, red shifts belong to the O–H (–287 to –320) and C=O (–11 to –21) bonds. Furthermore, in these complexes, blue shifts of O–Y (Y = F, Cl, Br) and O–Y (Y = I) were observed. In Type 3 complexes, the red shifts belong to C=O and O–Y bonds. The red shift of the O–H stretch was far greater than that of the O–Y, suggesting that they are stronger in hydrogen bonds than in halogen bonds.

**Table 3**. The selected vibrational stretching frequencies (cm–1) with corresponding intensities (values given in parentheses, km $mol^{-1}$) relative to the corresponding free molecules at the MP2/aug-cc-pVTZ and MP2/aug-cc-pVTZ(-PP) levels.

| | Type 1 | | Type 2 | | | Type 3 | |
|---|---|---|---|---|---|---|---|
| | $\nu$C=O | $\nu$O–H | $\nu$C=O | $\nu$O–H | $\nu$O–Y | $\nu$C=O | $\nu$?O–Y |
| FF | 1945(411) | 3435(656) | 1949(479) | 3480(670) | 984(1) | – | – |
| FCl | 1944(370) | 3424(656) | 1949(484) | 3429(760) | 673(13) | 1949(457) | 738(53)) |
| FBr | 1943(350) | 3443(689) | 1949(484) | 3488(760) | 773(13) | 1946(456) | 633(63) |
| FI | 1919(540) | 3471(560) | 1946(420) | 3506(590) | 774(18) | 1945(450) | 570(90) |
| ClF | 1924(675) | 3436(765) | 1925(683) | 3466(650) | 984(1) | – | – |
| ClCl | 1922(628) | 3415(827) | 1925(685) | 3470(740) | 774(8) | 1932(7) | 737(42) |
| ClBr | 1921(600) | 3423(785) | 1926(81) | 3488(713) | 675(8) | 1918(776) | 630(83) |
| ClI | 1971(70) | 3471(659) | 1921(545) | 3494(492) | 615(28) | 1921(809) | 569(99) |
| BrF | 1921(771) | 3436(798) | 1922(755) | 3465(627) | 983(1) | – | – |
| BrCl | 1919(724) | 3414(860) | 1922(755) | 3464(627) | 774(8) | 1930(841) | 736(46) |
| BrBr | 1918(694) | 3423(811) | 1918(752) | 3488(679) | 675(11) | 1924(898) | 633(17) |
| BrI | 1918(636) | 3413(682) | 1924(607) | 3496(469) | 611(11) | 1920(947) | 568(99) |
| IF | 1919(868) | 3419(867) | 1918(840) | 3444(636) | 983(1) | – | – |
| ICl | 1916(65) | 3394(946) | 1918(840) | 3447(704) | 775(9) | 1927(985) | 735(51) |
| IBr | 1917(653) | 3408(850) | 1918(839) | 3472(666) | 676(12) | 1920(995) | 630(45) |
| II | 1916(736) | 3452(768) | 1914(740) | 3473(605) | 619(17) | 1917(997) | 567(83) |

### 2.5. QTAIM analysis

QTAIM analysis was used to investigate the characteristics of the O$\cdots$H, X$\cdots$ Y, and O$\cdots$Y bond critical points (BCPs). Table 5 and Figure S1 represent the QTAIM results of the complexes. The QTAIM topological parameters include electronic density ($\rho$), Laplacian of electron density at BCP ($\nabla^2\rho$), total energy electron density (H), and –G/V ratio. The total energy electron density is obtained from Eq. (1):

$$H = G + V \tag{1}$$

Furthermore, the viral theorem can be concluded from Eq. (2):

**Table 4**. The selected vibrational stretching frequencies ($cm^{-1}$) with corresponding intensities (values given in parenthesis, km $mol^{-1}$) relative to corresponding free molecules at the MP2/aug-cc-pVTZ and MP2/aug-cc-pVTZ(-PP) levels.

| | $\upsilon_{C=O}$ | $\upsilon_{O-H}$ | $\upsilon_{O-Y}$ |
|---|---|---|---|
| $HC_3OF$ | 1957(495) | - | - |
| $HC_3OCl$ | 1942(706) | - | - |
| $HC_3OBr$ | 1940(799) | - | - |
| $HC_3OI$ | 1935(863) | - | - |
| HOF | - | 3764(1) | 979(1) |
| HOCl | - | 3773(81) | 766(12) |
| HOBr | - | 3774(93) | 662(16) |
| HOI | - | 3793(113) | 601(33) |

$$\frac{1}{4}\nabla^2_{BCP} = 2G + V \tag{2}$$

The kinetic electron energy density (G) is always positive, while the potential electron energy density (V) must be negative. In Eq. (2), the positive values of Laplacian of electron density at BCP shows that G is greater than V, suggesting depletion of charge density in the interatomic surface.[45] The negative value for $\nabla^2\rho$ shows the concentration of the electron charge in the interatomic surface (covalent bonds (shared interaction)).[46] The hydrogen bonds can be classified into three types: weak hydrogen bonds ($\nabla^2\rho$ and H $>$ 0), medium hydrogen bonds ($\nabla^2\rho > 0$ and H $<$ 0), and strong hydrogen bonds, where both $\nabla^2\rho$ and H $<$ 0).[47] The O$\cdots$H interactions in IF1, ICl1, IBr1, II1, FI2, ClI2, BrI2, IF2, ICl2, IBr2, and II2 have $\nabla^2\rho > 0$, H $> 0$, and –G/V $< 1$, showing that these interactions are partially covalent. These interactions in other complexes have –G/V higher than 1, suggesting that these interactions are noncovalent. For X$\cdots$Y in FF2, FI2, ClI2, and II2 systems BCPs were not observed. For X$\cdots$Y in FI3, BrI3, IBr3, and II3 systems, –G/V $< 1$ and $H_{BCP} > 0$, confirming this interaction has a partially covalent nature. In addition, O$\cdots$Y in FCl3, FBr3, ClCl3, ClBr3, ClI3, BrCl3, BrBr3, and ICl3 complexes has –G/V $> 1$, indicating a halogen bond interaction with a noncovalent characteristic.

### 2.6. NBO analysis

The NBO method was applied to identify the nature of the interaction between HOY (Y = halogen) and $HC_3OX$ (X = halogen) molecules, which were performed at the MP2/aug-cc-pVTZ and MP2/aug-cc-pVTZ(-PP) levels of theory. The data supplied in Table 6 represent the second-order perturbation energy ($E^{(2)}$) for donor–acceptor interactions between the selected orbitals. The interaction between the lone pair (LP) orbital of the oxygen atom (as donor) and the antibonding sigma orbital of the O–H bond (as acceptor) corresponds to the hydrogen bond. Moreover, the interactions between the LPs of the electron donors (LP (X), LP (Y), and LP (O)) and the antibonding sigma orbital of the electron acceptors (O–Y and C–X) are due to the halogen bond. It can be seen that the LP (O) $\rightarrow \sigma^*$ (O–H) orbital interaction is far stronger than the other orbital interaction. The LP(O) $\rightarrow \sigma^*$ (O–H) in Type 1 and 2 complexes is decreased by increasing the Y atomic number (Br $<$ Cl $<$ F). As can be seen from the results, $E^{(2)}$ values of the halogen bond in Type 3 complexes (X, Y = F, Cl,

**Table 5**. Topological parameters for the complexes between HOY and $HC_3OX$.

| | Type 1 | | | |
|---|---|---|---|---|
| | O···H BCPs | | | |
| | $\rho$ | $\nabla^2\rho$ | H | –G/V |
| FF | 0.0263 | 0.1755 | 0.0021 | 1.0530 |
| FCl | 0.0271 | 0.1742 | 0.0012 | 1.0317 |
| FBr | 0.0267 | 0.1687 | 0.0012 | 1.0301 |
| FI | 0.0334 | –0.1336 | 0.0015 | 1.0034 |
| ClF | 0.0264 | 0.1777 | 0.0021 | 1.0550 |
| ClCl | 0.0273 | 0.1766 | 0.0013 | 1.0313 |
| ClBr | 0.0269 | 0.1714 | 0.0012 | 1.0297 |
| ClI | 0.0337 | –0.1666 | 0.0028 | 1.0349 |
| BrF | 0.0265 | 0.1779 | 0.0021 | 1.0548 |
| BrCl | 0.0273 | 0.1765 | 0.0012 | 1.0312 |
| BrBr | 0.0270 | 0.1711 | 0.0012 | 1.0297 |
| BrI | 0.0337 | 0.1185 | 0.0034 | 1.0100 |
| IF | 0.0385 | 0.1056 | 0.0063 | 0.8363 |
| ICl | 0.0392 | 0.1080 | 0.0065 | 0.8372 |
| IBr | 0.0376 | 0.0964 | 0.0055 | 0.8516 |
| II | 0.0358 | 0.1085 | 0.0043 | 0.8796 |

**Table 5**. Continued.

| | Type 2 | | | | | | | |
|---|---|---|---|---|---|---|---|---|
| | O···H BCPs | | | | X···Y BCPs | | | |
| | $P$ | $\nabla^2\rho$ | H | –G/V | $\rho$ | $\nabla^2\rho$ | H | –G/V |
| FF | 0.0257 | 0.1739 | 0.0024 | 1.0621 | – | – | – | – |
| FCl | 0.0260 | 0.1790 | 0.0025 | 1.0656 | 0.0051 | 0.0240 | 0.0010 | 1.2894 |
| FBr | 0.0260 | 0.1793 | 0.0026 | 1.0629 | 0.0057 | 0.0252 | 0.0010 | 1.2682 |
| FI | 0.0330 | 0.1064 | 0.0028 | 0.9130 | – | – | – | – |
| ClF | 0.0260 | 0.1790 | 0.0025 | 1.0656 | 0.0051 | 0.0240 | 0.0010 | 1.2894 |
| ClCl | 0.0262 | 0.1783 | 0.0021 | 1.0521 | 0.0047 | 0.0201 | 0.0011 | 1.4074 |
| ClBr | 0.0262 | 0.1784 | 0.0021 | 1.0521 | 0.0052 | 0.0212 | 0.0011 | 1.3225 |
| ClI | 0.0336 | 0.1071 | 0.0030 | 0.9058 | – | – | – | – |
| BrF | 0.0253 | 0.1674 | 0.0020 | 1.0529 | 0.0036 | 0.0174 | 0.0006 | 1.2000 |
| BrCl | 0.0257 | 0.1738 | 0.0022 | 1.0564 | 0.0049 | 0.0203 | 0.0010 | 1.3928 |
| BrBr | 0.0257 | 0.1738 | 0.0022 | 1.0564 | 0.0054 | 0.0209 | 0.0010 | 1.3125 |
| BrI | 0.0335 | 0.1070 | 0.0030 | 0.9054 | 0.0060 | 0.0198 | 0.0009 | 1.3448 |
| IF | 0.0382 | 0.1067 | 0.0061 | 0.8432 | 0.0064 | 0.0253 | 0.0011 | 1.2750 |
| ICl | 0.0379 | 0.1093 | 0.0059 | 0.8497 | 0.0065 | 0.0212 | 0.0011 | 1.3548 |
| IBr | 0.0367 | 0.1046 | 0.0053 | 0.8679 | 0.0063 | 0.0205 | 0.0010 | 1.3226 |
| II | 0.0348 | 0.1091 | 0.0036 | 0.8947 | – | – | – | – |

**Table 5**. Continued.

| | Type 3 | | | |
|---|---|---|---|---|
| | O$\cdots$Y BCPs | | | |
| | $\rho$ | $\nabla^2\rho$ | H | -G/V |
| FF | – | – | – | – |
| FCl | 0.0173 | 0.0874 | 0.0022 | 1.1271 |
| FBr | 0.0232 | 0.1051 | 0.0003 | 1.0117 |
| FI | 0.0297 | 0.1030 | 0.0002 | 0.9924 |
| ClF | – | – | – | – |
| ClCl | 0.0894 | 0.0894 | 0.0022 | 1.1235 |
| ClBr | 0.0237 | 0.1078 | 0.0002 | 1.0075 |
| ClI | 0.0185 | 0.0875 | 0.0031 | 1.2064 |
| BrF | – | – | – | – |
| BrCl | 0.0178 | 0.0896 | 0.0022 | 1.1229 |
| BrBr | 0.0237 | 0.1072 | 0.0002 | 1.0075 |
| BrI | 0.0305 | 0.1044 | 0.0005 | 0.9814 |
| IF | – | – | – | – |
| ICl | 0.0185 | 0.0875 | 0.0031 | 1.2064 |
| IBr | 0.0348 | 0.1258 | 0.0037 | 0.6011 |
| II | 0.0425 | 0.1357 | 0.0044 | 0.8972 |

Br) are larger than those in the corresponding Type 2 complexes, indicating a strong halogen bond interaction in Type 3 complexes. Furthermore, the results obtained indicated these values in Type 3 complexes containing I are larger than those in the corresponding Type 2 complexes. Therefore, in these complexes the halogen bond interaction was stronger than that in Type 2. The value of charge transfer (CT) from $HC_3OX$ to HOY is given in Table 5. The value of CT in Type 1 and 2 complexes decreases with the rise in the Y atomic number (Br < Cl < F). However, an inverse trend was observed for Type 3 complexes, with CT increasing with elevation in the Y atomic number.

### 2.7. Conclusion

MP2/aug-cc-pVTZ and MP2/aug-cc-pVTZ(-PP) calculations were performed to study the interaction between HOY (Y = F, Cl, Br, and I) and $HC_3OX$ (X = F, Cl, Br, and I) molecules. Three configurations were obtained for the interaction of $HC_3OX$ with HOY molecules. They included hydrogen bond (Type 1), hydrogen and halogen bonds (Type 2), and halogen bond (Type 3). The results obtained suggested that hydrogen bonds between $HC_3OX$ and HOY were stronger in Type 1 complexes than in Type 2 complexes. Moreover, halogen bonds between $HC_3OX$ and HOY were stronger in Type 3 complexes than in Type 2 complexes. The H–O bonds showed red shifts with complex formation in Types 1 and 2, with more considerable shifts for Type 1 complexes. The O–Y bonds displayed red and blue shifts in the Type 2 and 3 complexes, respectively. The LP(O) $\rightarrow \sigma^*$(O–H) orbital interaction was far stronger than the other orbital interactions. The $E^{(2)}$ values of the hydrogen bond in the Type 1 complexes were larger than those in the Type 2 complexes according to the NBO analysis results. In addition, the $E^{(2)}$ of the halogen bond in Type 3 structures was greater than that in Type 2 complexes, suggesting a strong halogen bond interaction in the Type 3 complexes.

**Table 6**. Second-order perturbation energy ($E^{(2)}$, kcal/mol) and charge transfer (CT, e).

| | Type 1 | | Type 2 | | Type 3 | | |
|---|---|---|---|---|---|---|---|
| | LP(O) → σ*(O–H) | CT | LP(O) → σ*(O–Y) | CT | LP(O) → σ*(O–Y) | LP(O) → σ*(C–X) | CT |
| FF | 18.83 | 0.024 | – | – | 18.32 | – | 0.11 |
| FCl | 18.28 | 0.021 | 4.33 | 0.008 | 17.51 | – | 0.13 |
| FBr | 16.76 | 0.018 | 9.49 | 0.016 | 16.19 | – | 0.16 |
| FI | 14.35 | 0.014 | 16.90 | 0.031 | 13.29 | – | 0.26 |
| ClF | 19.42 | 0.025 | – | – | 19.3 | 0.06 | – |
| ClCl | 18.89 | 0.020 | 4.55 | 0.009 | 18.54 | 0.10 | – |
| ClBr | 17.41 | 0.018 | 9.97 | 0.017 | 17.03 | 0.12 | – |
| ClI | 14.66 | 0.013 | 17.62 | 0.032 | 13.65 | 0.06 | – |
| BrF | 19.42 | 0.024 | – | – | 16.99 | 0.19 | – |
| BrCl | 18.9 | 0.019 | 4.55 | 0.009 | 18.53 | 0.16 | – |
| BrBr | 17.38 | 0.016 | 9.99 | 0.017 | 16.99 | 0.19 | – |
| BrI | 14.62 | 0.012 | 17.64 | 0.032 | 13.54 | 0.09 | – |
| IF | 20.24 | 0.025 | – | – | 20.79 | 0.18 | 0.17 |
| ICl | 19.90 | 0.021 | 4.69 | 0.009 | 19.93 | 0.29 | 0.19 |
| IBr | 18.33 | 0.019 | 10.36 | 0.018 | 17.89 | 0.33 | 0.27 |
| II | 19.36 | 0.016 | 18.02 | 0.033 | 14.65 | 0.10 | 0.29 |

## 3. Computational details

In the present study, all calculations were performed with the Gaussian 03 software package.[48] The geometry optimizations of the complexes formed between the cyclopropenone and hypohalous acids (HOY with Y = halogen) were carried out using the MP2 method[49] with the aug-cc-pVTZ basis set for all atoms, except I, for which the MP2/aug-cc-pVTZ(-PP) basis set was used.[50] In the investigation, the MP2/aug-cc-pVTZ(-PP) level of theory was applied to calculate the interaction energies and stability for systems containing iodine.[51] The frequency calculations at the same level indicated that all the structures obtained were in good agreement with those of the energetic minima. The interaction energies were corrected for the BSSE with the counterpoise method by Boys and Bernardi.[52] MEP was calculated on the 0.001 electrons/Bohr$^3$ contour of the electronic density using the Wave Function Analysis–Surface Analysis Suite (WFA–SAS).[53] To characterize the bond properties of the complexes, QTAIM analysis was performed with the help of AIM2000[54] and AIMAll.[40] The NBO analysis accomplished with the NBO program[55] provided using Gaussian 03.

The uncorrected stabilization energies ($SE^{uncorr}$) were calculated by the following equation:

$SE^{uncorr}$ = Ecomplex – (E($HC_3OX$) + E(HOY))

Then by adding ΔZPE (zero-point correction energy) and BSSE to $SE^{uncorr}$, $SE^{cp}$ was obtained as

$SE^{cp} = SE^{uncorr} + \Delta ZPE + BSSE$

In the $SE^{cp}$ both the corrections ΔZPE and BSSE were carried out on stabilization energies.

## References


1. Okuda, T.; Yoneyama, Y.; Fujiwara, A.; Furumai, T. *J. Antibiotics* **1984**, *37*, 712-717.
2. Sakaki, S.; Musashi, S.; Ohkubo, K. *J. Am. Chem. Soc.* **1993**, *115*, 1515-1519.
3. Liu, L.; Xia, S.; Fang, W. H. *J. Phys. Chem. A* **2014**, *118*, 8977-8985.
4. Breslow, R.; Oda, M. *J. Am. Chem. Soc.* **1972**, *94*, 8647-8647.
5. Komatsu, K.; Kitagawa, T. *Chem. Rev.* **2003**, *103*, 1371-1428.
6. Elrob, S. A. Y.; Osman, O. I.; Aziz, S. G. *Mol. Phys.* **2011**, *109*, 1785-1795.
7. Ahmadvand, S.; Zaari, R. R.; Varganov, S. A. *Astrophys. J.* **2014**, *795*, 173-178.
8. Poloukhtine, A.; Popik, V. V. M. *J. Phys. Chem. A* **2006**, *110*, 1749-1757.
9. Fitzpatrick, N.; Fanning, M. *J. Mol. Struct.* **1976**, *33*, 257-263.
10. Werz, D. B.; Klatt, G. N.; Raskatov, J. A.; Ko¨ppel, H.; Gleiter, R. *Organometallics* **2009**, *28*, 1675-1682.
11. Nguyen, L. T.; Proft, F. De.; Nguyen, M. T.; Geerlings, P. *J. Chem. Soc. Chem. Commun.* **2001**, *2*, 898-905.
12. Nguyen, L. T.; Proft, F. De.; Nguyen, M. T.; Geerlings, P. *J. Org. Chem.* **2001**, *66*, 4316-4326.
13. Hobza, P.; Müller-Dethlefs, K. *Roy. Soc. Ch.* **2010**, *2*, 1-20.
14. Raju, R. K.; Bloom, J. W. G.; An, Y.; Wheeler, S. E. *ChemPhysChem.* **2011**, *12*, 3116-3130.
15. Seth, S. K.; Manna, P.; Singh, N. J.; Mitra, M.; Jana, A. D.; Das, A.; Choudhury, S. R.; Kar, T.; Mukhopadhyay, S.; Kim, K. S. *CrystEngComm.* **2013**, *15*, 1285-1288.
16. Alberto, M. E.; Mazzone, G.; Russo, N.; Sicilia, E. *J. Chem. Soc. Chem. Commun.* **2010**, *46*, 5894-5896.
17. Černý, J.; Hobza, P. *Phys. Chem. Chem. Phys.* **2007**, *9*, 5291-5303.
18. Mohan, N.; Suresh, C. H. *J. Phys. Chem.* **2014**, *118*, 1697-1705.
19. Grabowski, S. J. *Phys. Chem. Chem. Phys.* **2013**, *15*, 7249-7259.
20. Vatanparast, M. *Comput. Theor. Chem.* **2014**, *1048*, 77-83.
21. Wilcken, R.; Zimmermann, M. O.; Lange, A.; Joerger, A. C.; Boeckler, F. M. *J. Med. Chem.* **2013**, *56*, 1363-1388.
22. Shiraga, K.; Adachi, A.; Nakamura, M.; Tajima, T.; Ajito, K.; Ogawa, Y. *J. Chem. Phys.* **2017**, *146*, 102-105.
23. Vatanparast, M.; Taghizadeh, M. T.; Parvini, E. *J. Theor. Comput. Chem.* **2015**, *14*, 1550046-1550060.
24. Zabardasti, A.; Solimannejad, M. *J. Mol. Struct*: *THEOCHEM.* **2007**, *819*, 52-59.
25. Zabardasti, A.; Zare, N.; Arabpour, M. *Struct. Chem.* **2011**, *22*, 691-695.
26. Politzer, P.; Murray, J.; Clark, T. *Phys. Chem. Chem. Phys.* **2010**, *12*, 7748-7757
27. Metrangolo, P.; Murray, J. S.; Pilati, T.; Politzer, P.; Resnati, G.; Terraneo, G. *Cryst. Growth* **2011**, *11*, 4238-4246.
28. Valerio, G.; Raos, G.; Meille, S. V.; Metrangolo, P.; Resnati, G. *J. Phys. Chem. A* **2000**, *104*, 1617-1620.
29. Arunan, E.; Desiraju, G. R.; Klein, R. A.; Sadlej, J.; Scheiner, S.; Alkorta, S. I.; Clary, D. C.; Crabtree, R. H.; Dannenberg, J. J.; Hobza, P.; et al. *Pure Appl. Chem.* **2011**, *83*, 1619-1627.
30. Li, Q.; Zhu, H.; Zhuo, H.; Yang, X.; Li, W.; Cheng, J. *Spectrochim. Acta A Mol. Biomol. Spectrosc.* **2014**, *132*, 271-277.
31. Li, Q.; Xu, X.; Liu, T.; Jing, B.; Li, W.; Cheng, J; Gong, B; Sun, J. *Phys. Chem. Chem. Phys.* **2010**, *12*, 6837-6843.
32. Sanchez-Sanz, G.; Trujillo, C.; Alkorta, I.; Elguero, J. *Phys. Chem. Chem. Phys.* **2012**, *14*, 9880-9889.
33. An, X.; Yang, X.; Xiao, B.; Cheng, J.; Li, Q. *Mol Phys. 2***017**, *115*, 1614-1623.
34. Blanco, F.; Alkorta, I.; Solimannejad, M.; Elguero, J. *J. Phys. Chem. A* **2009**, *113*, 3237-3244.
35. Ghanty, T. K.; Ghosh, S. K. *J. Phys. Chem. A* **1997**, *27*, 5022-5025.
36. Zabardasti, A.; Sharifi-rad, A.; Kakanejadifard, A. *Spectrochim. Acta A* **2015**, *151*, 746-759.

37. Li, Q.; Zhu, H.; Yang, X.; Li, W.; Cheng, J. *Spectrochim. Acta A* **2014**, *132*, 271-277.
38. Alkorta, I.; Blanco, F.; Solimannejad, M.; Elguero, J. *J. Phys. Chem. A* **2008**, *112*, 10856-10863.
39. Zabardasti, A.; Kakanejadifard, A.; Goudarziafshar, H.; Salehnassaj, M.; Zohrehband, Z.; Jaberansari, F.; Solimannejad, M. *Comput. Theor. Chem.* **2013**, *1014*, 1-7.
40. Bader, R. F. W. Atoms in Molecules: a Quantum Theory. Clarendon: Oxford, UK, 1990.
41. Politzer, P.; Murray, J. S. *Phys. Chem. Chem. Phys.* **2013**, *15*, 11178-11189.
42. Reed, A. E.; Curtiss, L. A.; Weinhold, F. *Chem. Rev.* **1988**, *88*, 899-926.
43. Sánchez-Sanz, G.; Trujillo, C.; Solimannejad, M.; Alkorta, I.; Elguero, J. *Phys. Chem. Chem. Phys.* **2013**, *15*, 14310-14318.
44. Bondi, A. *J. Phys. Chem.* **1964**, *68*, 441-451.
45. Ziółkowski, M.; Grabowski, S. J.; Leszczynski, J. *J. Phys. Chem. A* **2006**, *110*, 6514-6521.
46. Zhang, X.; Li, X.; Zeng, Y.; Meng, L.; Zheng, S. *Int. J. Quantum. Chem.* **2014**, *114*, 400-408.
47. Rozas, I.; Alkorta, I.; Elguero, J. *J. Am. Chem. Soc.* **2000**, *122*, 11154-11161.
48. Frisch, M.; Trucks, G; Schlegel, H.; Scuseria, G.; Robb, M.; Cheeseman, J.; Montgomery Jr, J.; Vreven, T.; Kudin, K.; Burant, J. Gaussian 03, revision c. 02; Gaussian, Inc.: Wallingford, CT, USA, 2004.
49. Cremer, D. *Comput. Mol. Sci.* **2011**, *1*, 509-530.
50. Esrafili, M. D.; Mohammadirad, N. *J. Mol. Model.* **2013**, *19*, 2559-2566.
51. Esrafili, M. D.; Solimannejad, M. N. *J. Mol. Model.* **2013**, *19*, 3767-3774.
52. Boys, S. F.; Bernardi, F. D. *Mol. Phys.* **1970**, *19*, 553-566.
53. Bulat, F. A.; Toro-Labbé, A.; Brinck, T.; Murray, J. S.; Politzer, P. *J. Mol. Model.* **2010**, *16*, 1679-1691.
54. Biegler Konig, F.; Schonbohm, J. *J. Comput. Chem.* **2001**, *22*, 545-559.
55. Glendening, E. D.; Weinhold, F. *J. Comput. Chem.* **1998**, *19*, 593-609.

**Supplementary**

**Table S1.** The change in selected vibrational stretching frequencies ($cm^{-1}$) relative to obtained complexes at the MP2/aug-cc-pVTZ level.

| | Type 1 | | Type 2 | | | Type 3 | |
|---|---|---|---|---|---|---|---|
| | $\Delta\upsilon_{C=O}$ | $\Delta\upsilon_{O-H}$ | $\Delta\upsilon_{C=O}$ | $\Delta\upsilon_{O-H}$ | $\Delta\upsilon_{O-Y}$ | $\Delta\upsilon_{C=O}$ | $\Delta\upsilon_{O-Y}$ |
| FF | –12 | –328 | –8 | –294 | 5 | – | – |
| FCl | –13 | –349 | –8 | –275 | 11 | –7 | –28 |
| FBr | –14 | –331 | –8 | –289 | 12 | –11 | –29 |
| FI | –38 | –332 | –11 | –287 | 15 | –12 | –31 |
| ClF | –18 | –327 | –16 | –297 | 5 | – | – |
| ClCl | –20 | –359 | –16 | –303 | 8 | –10 | –29 |
| ClBr | –21 | –351 | –16 | –286 | 13 | –16 | –32 |
| ClI | 29 | –322 | –21 | –299 | 14 | –20 | –32 |
| BrF | –18 | –328 | –17 | –289 | 5 | – | – |
| BrCl | –20 | –359 | –17 | –304 | 8 | –10 | –29 |
| BrBr | –21 | –351 | –22 | –286 | 12 | –16 | –29 |
| BrI | –21 | –380 | –16 | –297 | 10 | –21 | –33 |
| IF | –21 | –344 | –17 | –319 | 5 | – | – |
| ICl | –18 | –379 | –17 | –326 | 9 | –8 | –31 |
| IBr | –20 | –366 | –21 | –302 | 13 | –15 | –32 |
| II | –18 | –341 | –20 | –320 | 18 | –18 | –34 |

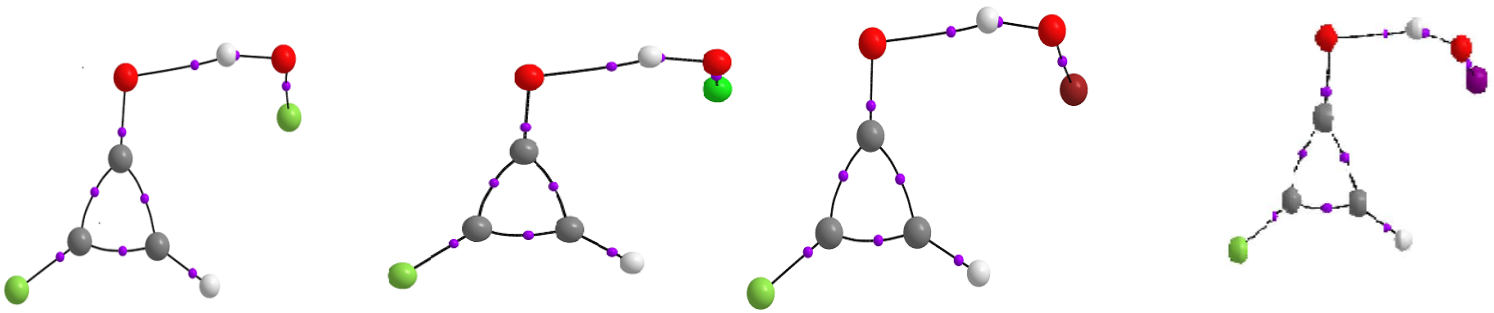

**Type 1**

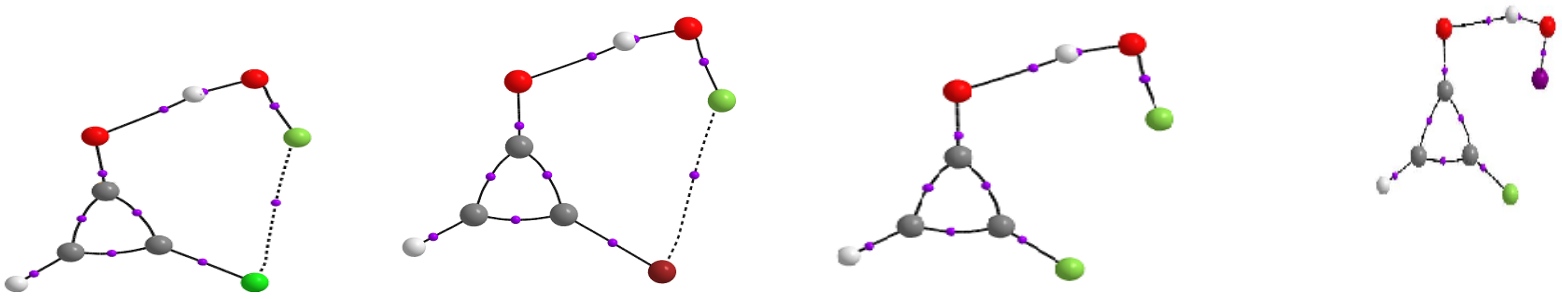

**Type 2**

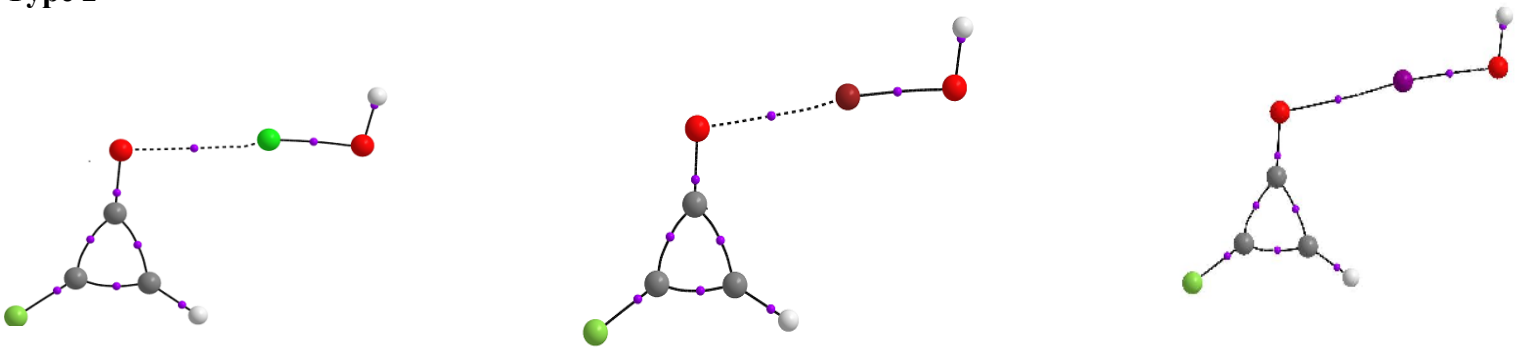

**Type 3**

**Supplementary Figure S1.** The Molecular graphs between $HC_3OX$ and HOY (X=Y=F, Cl, Br and I) at MP2/aug-cc-pVTZ level.